molbank

MDPI

Short Note

[4,6-Di-*tert*-butyl-*N*-(2,6-Dimethylphenyl)-*o*-Amidophenolato][4,6-Di-*tert*-butyl-*N*-(2,6-Dimethylphenyl)-*o*-Iminobenzosemiquinolato](2,2′-Bipyridyl)Indium(III)

Irina V. Ershova, Anton V. Cherkasov and Alexandr V. Piskunov *

G. A. Razuvaev Institute of Organometallic Chemistry of Russian Academy of Sciences, 49 Tropinina str., 603950 Nizhny Novgorod, Russia; irina@iomc.ras.ru (I.V.E.); ach@iomc.ras.ru (A.V.C.)
* Correspondence: pial@iomc.ras.ru

Abstract: A six-coordinated indium(III) complex (AP^{Me})($imSQ^{Me}$)In(bipy) (**1**), bearing two types of redox-active ligands—mono- ($imSQ^{Me}$) and dianion (AP^{Me}) of 4,6-di-*tert*-butyl-*N*-(2,6-dimethylphenyl)-*o*-iminobenzoquinone and 2,2′-bipyridyl—was synthesized and characterized in detail. The intense, well-resolved ESR spectrum of **1** in dichloromethane solution clearly indicates the spin density delocalization between both AP and imSQ ligands. The UV-vis spectrum of **1** possesses an absorption band in the NIR region. The molecular structure of compound **1** was established by single-crystal X-ray diffraction analysis.

Keywords: indium; redox-active ligand; *o*-amidophenolate; *o*-iminobenzosemiquinolate; bipyridyl; charge transfer; ESR; X-ray diffraction

check for updates

Citation: Ershova, I.V.; Cherkasov, A.V.; Piskunov, A.V. [4,6-Di-*tert*-butyl-*N*-(2,6-Dimethylphenyl)-*o*-Amidophenolato][4,6-Di-*tert*-butyl-*N*-(2,6-Dimethylphenyl)-*o*-Iminobenzosemiquinolato](2,2′-Bipyridyl)Indium(III). *Molbank* **2023**, *2023*, M1660. https://doi.org/10.3390/M1660

Academic Editor: Kristof Van Hecke

Received: 19 May 2023
Revised: 1 June 2023
Accepted: 2 June 2023
Published: 6 June 2023

1. Introduction

Plenty of chromophore systems include rich classes of intramolecular charge transfer dyes represented by organic [1–4], polymer [5,6], organometallic [7], and coordination compounds [8]. A design of metal complexes, which contains both donor and acceptor organic parts coordinated to the metal center and can act as ligand-to-ligand charge-transfer (LL´CT) chromophores, is one of the actual trends in modern chemistry [9–13]. Since the structure and therefore absorption profile, redox potentials, and molecular polarity of LLCT complexes can be tuned easily, these compounds can find application in photochemical charge-transfer and nonlinear optics [14–20]. Currently, the donor–acceptor complexes of transition metals (Ni [21–26], Pd [25,27–29], Pt [20,25,28–33]) with redox-active ligands are the most studied and perspective compounds for application to dye-sensitized solar cells. The development of sibling LL´CT chromophores based on main-group metals seems exceedingly attractive since it would allow one to cheapen the potential production process. Recently, we have synthesized several LL´CT gallium complexes, bearing the quinone-type redox-active ligands as donor and 2,2′-bipyridyl as acceptor [34–36]. Furthermore, in the complexes with two differently charged *o*-quinone ligands, the absorption maximum shifts to the near IR region [35]. Here, we report the synthesis and characterization of a new indium(III) complex containing *o*-iminobenzoquinone ligands in different redox states (radical anion and dianion) along with neutral 2,2′-bipyridyl in the metal coordination sphere.

2. Results

The exchange reaction between equimolar quantities of anhydrous InI_3, 2,2´-bipyridyl, and sodium salts of singly and doubly reduced 4,6-di-*tert*-butyl-*N*-(2,6-dimethylphenyl)-*o*-iminobenzoquinone ((imSQ^{Me})Na and ((AP^{Me})Na_2, respectively) leads to the formation of the hexacoordinated heteroleptic indium complex (AP^{Me})($imSQ^{Me}$)In(bipy) (**1**) (Scheme 1).

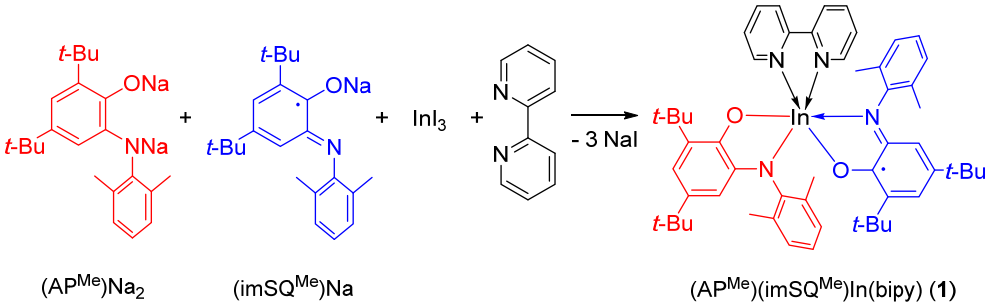

Scheme 1. Synthesis of Complex **1**.

Complex **1** is extremely sensitive to atmospheric oxygen and moisture, both in solution and in the crystalline state. It is highly soluble in THF, has moderate solubility in dichloromethane, and is insoluble in toluene and saturated hydrocarbons. The composition and structure of **1** were established by spectroscopic methods (IR, ESR, UV-Vis-NIR spectroscopy) as well as by elemental and X-ray diffraction analyses (Supplementary Materials).

The IR spectrum of **1** is characterized by a set of lines due to the presence of two different charged *o*-iminobenzoquinone fragments along with the bipyridyl ligand. The presence of two differently charged *o*-iminobenzoquinone ligands in **1** was also detected by ESR spectroscopy. The hyperfine structure of the ESR spectrum of **1** (Figure 1) is caused by hyperfine coupling of unpaired electron with magnetic nuclei ^{115}In (95.7%, I = 9/2, μ_N = 5.534) [37], two equivalent protons ^{1}H (99.98%, I = 1/2, μ_N = 2.7928) [37] and two equivalent nitrogen atoms ^{14}N (99.63%, I = 1, μ_N = 0.4037) [37] of both *o*-iminobenzoquinone ligands. The detected intense signal specifies the fast (on the ESR time scale) migration of the unpaired electron between radical anion and dianion redox-active ligands.

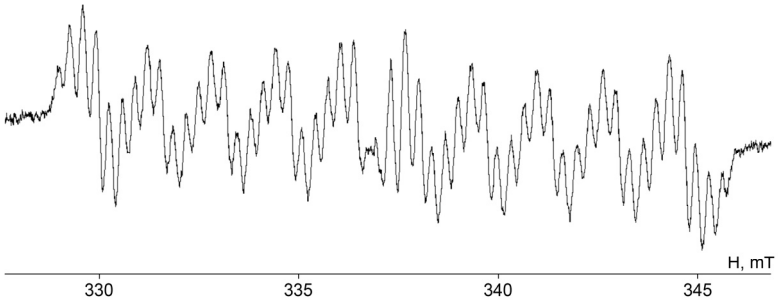

Figure 1. ESR spectrum (g_i = 2.0069, $a_i(^{115}In)$ = 1.47 mT, $a_i(2^{14}N)$ = 0.34 mT, $a_i(2^{1}H)$ = 0.29 mT) of **1** in dichloromethane at 290 K.

The electronic absorption spectrum of complex **1** was recorded in the range of 200–1100 nm in dichloromethane at 298 K (Figure 2). Besides high-intensity absorption bands in the near UV range (235 nm, ε = 25137; 289 nm, ε = 17443; 311 nm, ε = 15808) corresponding to the π—π* transitions in aromatic compounds, the visible and near-IR regions contain a broad low-intensity absorption band (765 nm, ε = 907), corresponding to the LL'CT between AP and imSQ redox-active ligands.

Despite the low reflectivity of crystalline samples **1** (see experimental section for details), we succeeded in selecting a crystal sample grown from CH_2CL_2/hexane solution and to carry out single-crystal X-ray diffraction (SC XRD) study. According to SC XRD data, **1** crystallizes in orthorhombic *Pbca* space group with unique complex molecule in asymmetric unit. The asymmetric unit also contains one solvent hexane molecule lying on the inversion center; thus, **1** crystallizes as a solvate **1**·$\frac{1}{2}$hexane.

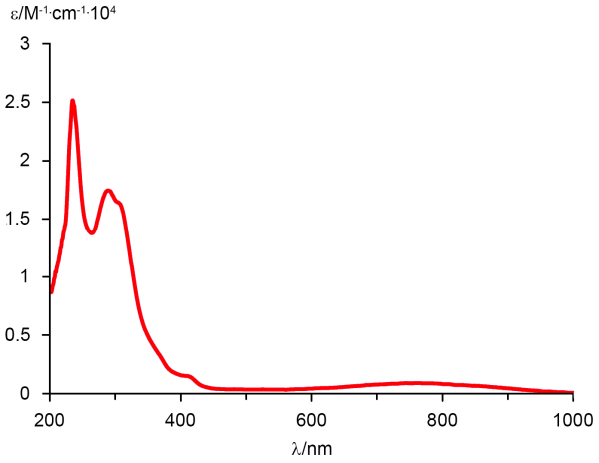

Figure 2. Electronic absorption spectrum of **1** recorded at 298 K in CH_2Cl_2 at C = 10^{-4} mol L^{-1}.

Coordination environment of In^{3+} cation in **1** is represented by a distorted octahedron with nitrogen and oxygen atoms at its vertices (Figure 3). The arrangement of *o*-iminobenzoquinone ligands in **1** results in the *trans* position of the nitrogen atoms with aryl substi-tuents. The dihedral angle between mean planes of metallacycles InOCCN is 61.2(2)°.

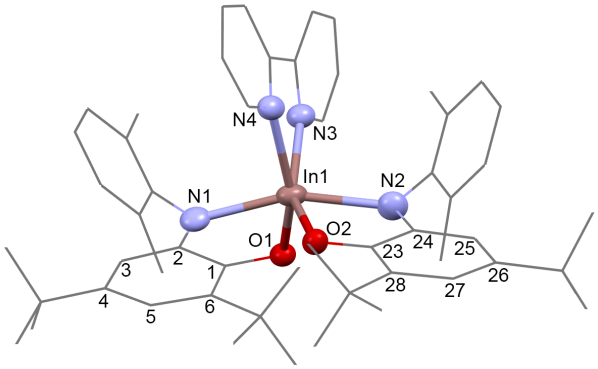

Figure 3. Molecular structure of **1** (anisotropic displacement ellipsoids of heteroatoms drawn at the 30% probability level; H atoms are omitted for clarity).

The redox states of *o*-iminobenzoquinone ligands in **1** are of particular interest. The C(1)-O(1), C(2)-N(2), and C(1)-C(2) bond lengths are 1.376(10) Å, 1.386(9), and 1.427(11) Å, respectively, and comparable with those distances in indium(III) complexes with di-anionic *o*-iminobenzoquinone ligand (AP)InI(TMEDA) (C-O 1.351(2) Å; C-N 1.402(3) Å; C-C 1.425(3) Å) (CCDC 770657) [38] and $[In(AP)_2]^-[Na(DME)_3]^+$ (C-O 1.355(3), 1.364(3) Å; C-N 1.394(3), 1.397(3) Å; C-C 1.423(3), 1.432(3) Å) (CCDC 928221) [39]. The metallacycle In(1)O(1)C(1)C(2)N(1) is not planar; the dihedral angle between the O(1)In(1)N(1) and O(1)C(1)C(2)N(1) planes is 164.9(5)°. The In(1)-O(1) and In(1)-N(1) distances are 2.101(5) Å and 2.250(8) Å, respectively. While the In-O in **1** is slightly shorter than similar distances in previously reported six-coordinated In^{3+} complexes with radical anion *o*-iminobenzoquinone ligands $(imSQ)_2InSS$ (2.1700(10), 2.1688(10) Å), $(imSQ)InCl_2(TMEDA)$ (2.163(3) Å) (CCDC 1002475, 1002476) [40], $(imSQ)InI_2(TMEDA)$ (2.1459(17) Å), (CCDC 770659) [38], the In-N distances in **1** are comparable to analogues characteristics of these complexes (2.2517(12)-2.271(2) Å), which can be explained by the steric saturation of the In^{3+} cation coordination sphere in **1**. Indeed, the geometry of the 2,2′-bipyridyl moiety in **1** is distorted (torsion angle N-C-C-N is 17.6(9)°) comparing to the related six-coordinated indium complex with *o*-quinone ligands (Cat)In(SQ)(bipy) (3.53(7)°) (CCDC 780470) [41], and the In-N_{bipy} bond lengths in **1** (2.283(7), 2.326(7) Å) are noticeably longer than in

(Cat)In(SQ)(bipy) (2.276(2), 2.279(2) Å). Thus, the O(1)N(1)-ligand state is characterized as dianionic.

While the bond lengths N(2)-C(24) (1.386(10) Å) and C(23)-C(24) (1.422(12) Å) are comparable to the distances N(1)-C(2) and C(1)-C(2), the bond length O(2)-C(23) is 1.307(10) Å and noticeably shorter than O(1)-C(1). The metallacycle In(1)O(2)C(23)C(24)N(2) is more planar than in the other ligand; the dihedral angle between the O(2)In(1)N(2) and O(2)C(23) C(24)N(2) planes is 171.3(5)°. The In(1)-O(2) and In(1)-N(2) bond lengths are 2.090(5) Å and 2.300(8) Å, respectively. Despite distortions in the geometry of the metallocycle, this ligand can be characterized as a radical anion.

The analysis of bond lengths in *o*-iminobenzoquinone ligands in **1** was carried out using metrical oxidation state (MOS) approach [42] as well. The calculated MOS are -1.95 ± 0.21 for O(1)N(1)-ligand and -1.52 ± 0.19 for O(2)N(2)-ligand and match satisfactorily the formal oxidation state of ligands supposed for the electronic structure of **1**.

3. Materials and Methods

All operations for the synthesis of (AP^{Me})($imSQ^{Me}$)In(bipy) (**1**) were carried out in the absence of atmospheric oxygen and moisture. Solvents were purified using standard methods [43]. Commercial reagents (sodium, indium, 2,2′-bipyridyl) were purchased from Aldrich. Anhydrous indium(III) iodide was obtained by stirring an excess of the metal with a stoichiometric amount of iodine in dry diethyl ether until the solution became colorless and used in situ. The sodium and disodium salts of 4,6-di-*tert*-butyl-*N*-(2,6-dimethylphenyl)-*o*-iminobenzoquinone (($imSQ^{Me}$)Na and (AP^{Me})Na_2, respectively) were synthesized from *o*-iminobenzoquinone (imQ^{Me}) [44] and used in situ. To obtain (AP^{Me})Na_2 imQ^{Me} (0.1 g, 0.31 mmol) was stirred with an excess of sodium dispersion (1.5 g, 65.2 mmol) in THF (20 ml) until solution color became light yellow. The oxidation of (AP^{Me})Na_2 (0.31 mmol) by the equivalent of imQ^{Me} (0.1 g, 0.31 mmol) leads to the formation of deep blue ($imSQ^{Me}$)Na (0.62 mmol). Elemental analysis was performed using the elemental analyzer Elementar Vario EL cube. The IR spectrum was recorded on an FSM 1201 spectrometer in a Nujol (range: 4000–400 cm^{-1}). The ESR spectrum was obtained using a Bruker Magnettech ESR5000 spectrometer. The electronic spectrum of **1** was recorded on a Perkin–Elmer Lambda 25 UV/Vis spectrometer (range: 220–1100 nm) at room temperature.

3.1. Synthesis of **1**

A freshly prepared bright-yellow solution of (AP^{Me})Na_2 (0.62 mmol) in THF (10 mL) was added to a colorless solution of InI_3 (0.62 mmol) in the same solvent (5 mL), and herewith the reaction mixture became brownish-orange. After that, the deep blue solution of ($imSQ^{Me}$)Na (0.62 mmol) in THF was added thereto upon stirring, and the color of the reaction mixture transformed to deep-green one. Finally, after 2,2′-bipyridyl addition (97 mg, 0.62 mmol), the reaction was kept at room temperature for 30 min. Then solvent was evaporated under reduced pressure, dry residue dissolved in dichloromethane (30 mL), and the reaction mixture was separated from the NaI precipitate by filtration. The green filtrate was concentrated and mixed up with hexane (10 mL) to provide better product precipitation. The pale-green precipitate of **1** was collected by filtration and dried in a vacuum (yield 75%). Elemental analysis: Calculated (%) for $C_{54}H_{66}InN_4O_2$: C 70.66, H 7.25, N 6.10; Found (%): C 70.89, H 7.43, N 5.99. UV–vis (CH_2Cl_2) nm (ε, M^{-1} cm^{-1}): 235 (25,137), 289 (17,443), 311sh (15,808), 418sh (1322), 765 (907). IR (Nujol, KBr) cm^{-1}: 1605 (m), 1598 (s), 1580 (m), 1568 (m), 1547 (m), 1355 (s), 1331 (s), 1316 (m), 1284 (s), 1259 (s), 1247 (s), 1232 (s), 1204 (m), 1173 (m), 1159 (m), 1126 (w), 1116 (w), 1097 (m), 1061 (w), 1042 (w), 1020 (s), 989 (m), 918 (w), 913 (w), 887 (m), 868 (m), 858 (w), 842 (w), 830 (w), 817 (w), 760 (s), 735 (m), 650 (m), 631 (w), 621 (w), 603 (w), 541 (w), 529 (w), 494 (w), 480 (w).

3.2. Single-Crystal X-ray Structure Analysis

The SC XRD data for **1** were collected with *Rigaku OD Xcalibur E* diffractometer ($Mo_{K\alpha}$-radiation, ω-scans technique, λ = 0.71073 Å, T = 298.0(2) K) using *CrysAlis*^{Pro} [45] software

package. Analytical numeric absorption correction using a multifaceted crystal model was performed. The structures were solved via intrinsic phasing algorithm and were refined by full-matrix least squares on F^2 for all data using *SHELX* [46,47]. All non-hydrogen atoms in **1** were found from Fourier syntheses of electron density and refined anisotropically. All hydrogen atoms were placed in calculated positions and refined isotropically in the "riding" model with $U(H)_{iso} = 1.2U_{eq}$ of their parent atoms ($U(H)_{iso} = 1.5U_{eq}$ for methyl groups).

Crystal data for **1**: $C_{54}H_{66}InN_4O_2 \cdot \frac{1}{2}C_6H_{14}$, M = 961.01, *Pbca*, a = 17.4861(16) Å, b = 23.472(2) Å, c = 26.342(4) Å, V = 10812(2) Å^3, Z = 8, d_{calc} = 1.181 g/cm^3. Green plate single crystal with dimensions 0.19 × 0.16 × 0.08 mm was selected and intensities of 55,759 reflections were collected (μ = 0.479 mm^{-1}, θ_{max} = 25.03°). After merging of equivalence reflections and absorption corrections, 9532 independent reflections (R_{int} = 0.2068) were used for the structure solution and refinement. Final R factors R_1 = 0.0865 [for 3263 reflections with $F^2 > 2\sigma(F^2)$], wR_2 = 0.2356 (for all reflections), S = 1.011, and largest diff. peak and hole are 0.52 and −0.38 e/Å^3, respectively.

Supplementary Materials: The following materials are available online: crystallographic information; IR, ESR, electronic spectroscopy data of compound **1**.

Author Contributions: Investigation, project administration, writing—original draft, I.V.E.; formal analysis, A.V.C.; supervision, writing—review and editing, A.V.P. All authors have read and agreed to the published version of the manuscript.

Funding: This research was funded by the Council for Grants of the President of Russian Federation (I. V. Ershova, Scholarship of the President of the Russian Federation for young scientists and graduate students carrying out promising research and development in priority areas of modernization of the Russian economy, grant number SP-1538.2021.1).

Data Availability Statement: CCDC 2263228 contains the supplementary crystallographic data for this paper. These data are provided free of charge by the Cambridge Crystallographic Data Centre: ccdc.cam.ac.uk/structures.

Acknowledgments: X-ray diffraction studies were carried out within the framework of the state assignment using the scientific equipment of the Center for Collective Use "Analytical Center of the Institute of Organometallic Chemistry of the Russian Academy of Sciences", functioning with the financial support from the Ministry of Science and Higher Education of the Russian Federation (program "Ensuring the development of the material and technical infrastructure of centers for the collective use of scientific equipment", Unique identifier RF—2296.61321X0017, agreement number 075-15-2021-670).

Conflicts of Interest: The authors declare no conflict of interest.

References

1. Qian, G.; Wang, Z.Y. Near-Infrared Organic Compounds and Emerging Applications. *Chem. Asian J.* **2010**, *5*, 1006–1029. [CrossRef]
2. Gerasimova, T.P.; Shamsieva, A.V.; Strel'nik, I.D.; Katsyuba, S.A.; Musina, E.I.; Karasik, A.A.; Sinyashin, O.G. Study of the structures and photophysical properties of 1,3-diaza-5-phosphacyclohexanes using density functional theory and optical spectroscopy. *Russ. Chem. Bull.* **2020**, *69*, 449–457. [CrossRef]
3. Kalinin, A.A.; Sharipova, S.M.; Islamova, L.N.; Fazleeva, G.M.; Busyurova, D.N.; Sharipova, A.V.; Fominykh, O.D.; Balakina, M.Y. Chromophores with quinoxaline core in π-bridge and aniline or carbazole donor moiety: Synthesis and comparison of their linear and nonlinear optical properties. *Russ. Chem. Bull.* **2022**, *71*, 1009–1018. [CrossRef]
4. Wu, J.; Shi, Z.; Zhu, L.; Li, J.; Han, X.; Xu, M.; Hao, S.; Fan, Y.; Shao, T.; Bai, H.; et al. The Design and Bioimaging Applications of NIR Fluorescent Organic Dyes with High Brightness. *Adv. Opt. Mater.* **2022**, *10*, 2102514. [CrossRef]
5. Marechal, E. Polymeric dyes—Synthesis, properties and uses. *Prog. Org. Coat.* **1982**, *10*, 251–287. [CrossRef]
6. Peng, D.; Tang, G.; Hu, J.; Xie, Q.; Zhou, J.; Zhang, W.; Zhong, C. Novel D–π–A dye sensitizers of polymeric metal complexes with triphenylamine or carbazole derivatives as donor for dye-sensitized solar cells: Synthesis, characterization and application. *Polym. Bull.* **2015**, *72*, 653–669. [CrossRef]
7. Ho, C.-L.; Li, H.; Wong, W.-Y. Red to near-infrared organometallic phosphorescent dyes for OLED applications. *J. Organomet. Chem.* **2014**, *751*, 261–285. [CrossRef]
8. Saygili, Y.; Stojanovic, M.; Flores-Díaz, N.; Zakeeruddin, S.M.; Vlachopoulos, N.; Grätzel, M.; Hagfeldt, A. Metal coordination complexes as redox mediators in regenerative dye-sensitized solar cells. *Inorganics* **2019**, *7*, 30. [CrossRef]

9. Kim, D.; Gra, T.G.; Teets, T.S. Heteroleptic copper(i) charge-transfer chromophores with panchromatic absorption. *Chem. Commun.* **2022**, *58*, 11446–11449. [CrossRef]
10. Pashanova, K.I.; Ershova, I.V.; Trofimova, O.Y.; Rumyantsev, R.V.; Fukin, G.K.; Bogomyakov, A.S.; Arsenyev, M.V.; Piskunov, A.V. Charge Transfer Chromophores Derived from 3d-Row Transition Metal Complexes. *Molecules* **2022**, *27*, 8175. [CrossRef]
11. Li, G.; Jiang, Z.; Tang, M.; Jiang, X.; Tu, H.; Zhu, S.; Liu, R.; Zhu, H. Synthesis, Photophysics and Tunable Reverse Saturable Absorption of Bis-Tridentate Iridium(III) Complexes via Modification on Diimine Ligand. *Molecules* **2023**, *28*, 566. [CrossRef]
12. Shultz, D.A.; Stephenson, R.; Kirk, M.L. Dinuclear ligand-to-ligand charge transfer complexes. *Dalton Trans.* **2023**, *52*, 1970–1976. [CrossRef] [PubMed]
13. Younus, M.; Valandro, S.; Gobeze, H.B.; Ahmed, S.; Schanze, K.S. Wavelength and solvent controlled energy and charge transfer in donor-acceptor substituted platinum acetylide complexes. *J. Photochem. Photobiol. A Chem.* **2023**, *435*, 114303. [CrossRef]
14. Cummings, S.D.; Cheng, L.-T.; Eisenberg, R. Metalloorganic Compounds for Nonlinear Optics: Molecular Hyperpolarizabilities of M(diimine)(dithiolate) Complexes (M = Pt, Pd, Ni). *Chem. Mater.* **1997**, *9*, 440–450. [CrossRef]
15. Base, K.; Tierney, M.T.; Fort, A.; Muller, J.; Grinstaff, M.W. On the Second-Order Nonlinear Optical Structure−Property Relationships of Metal Chromophores. *Inorg. Chem.* **1999**, *38*, 287–289. [CrossRef]
16. Bonneval, B.G.-d.; Ching, K.I.M.-C.; Alary, F.; Bui, T.-T.; Valade, L. Neutral d8 metal bis-dithiolene complexes: Synthesis, electronic properties and applications. *Coord. Chem. Rev.* **2010**, *254*, 1457–1467. [CrossRef]
17. Deplano, P.; Pilia, L.; Espa, D.; Mercuri, M.L.; Serpe, A. Square-planar d8 metal mixed-ligand dithiolene complexes as second order nonlinear optical chromophores: Structure/property relationship. *Coord. Chem. Rev.* **2010**, *254*, 1434–1447. [CrossRef]
18. Archer, S.; Weinstein, J.A. Charge-separated excited states in platinum(II) chromophores: Photophysics, formation, stabilization and utilization in solar energy conversion. *Coord. Chem. Rev.* **2012**, *256*, 2530–2561. [CrossRef]
19. Bozic-Weber, B.; Constable, E.C.; Housecroft, C.E. Light harvesting with Earth abundant d-block metals: Development of sensitizers in dye-sensitized solar cells (DSCs). *Coord. Chem. Rev.* **2013**, *257*, 3089–3106. [CrossRef]
20. Scattergood, P.A.; Jesus, P.; Adams, H.; Delor, M.; Sazanovich, I.V.; Burrows, H.D.; Serpa, C.; Weinstein, J.A. Exploring excited states of Pt(II) diimine catecholates for photoinduced charge separation. *Dalton Trans.* **2015**, *44*, 11705–11716. [CrossRef]
21. Kramer, W.W.; Cameron, L.A.; Zarkesh, R.A.; Ziller, J.W.; Heyduk, A.F. Donor–Acceptor Ligand-to-Ligand Charge-Transfer Coordination Complexes of Nickel(II). *Inorg. Chem.* **2014**, *53*, 8825–8837. [CrossRef]
22. Bubnov, M.P.; Teplova, I.A.; Druzhkov, N.O.; Fukin, G.K.; Cherkasova, A.V.; Cherkasov, V.K. Catecholato complexes of cobalt and nickel with 1,4-disubstituted-1,4-diazabutadiens-1,3 and 1,2-bis(diphenylphosphino)ethane. *J. Chem. Sci.* **2015**, *127*, 527–535. [CrossRef]
23. Cameron, L.A.; Ziller, J.W.; Heyduk, A.F. Near-IR absorbing donor–acceptor ligand-to-ligand charge-transfer complexes of nickel(II). *Chem. Sci.* **2016**, *7*, 1807–1814. [CrossRef] [PubMed]
24. Yang, H.; Zhao, Y.; Liu, B.; Su, J.-H.; Fedushkin, I.L.; Wua, B.; Yang, X.-J. Noninnocent ligands: Heteroleptic nickel complexes with α-diimine and 1,2-diketone derivatives. *Dalton Trans.* **2017**, *46*, 7857–7865. [CrossRef] [PubMed]
25. Yamada, S.; Matsumoto, T.; Chang, H.-C. Impact of Group 10 Metals on the Solvent-Induced Disproportionation of o-Semiquinonato Complexes. *Chem. Eur. J.* **2019**, *25*, 8268–8278. [CrossRef] [PubMed]
26. Pashanova, K.I.; Bitkina, V.O.; Yakushev, I.A.; Arsenyev, M.V.; Piskunov, A.V. Square-Planar Heteroleptic Complexes of α-Diimine-NiII-Catecholate Type: Intramolecular Ligand-to-Ligand Charge Transfer. *Molecules* **2021**, *26*, 4622. [CrossRef]
27. Kokatam, S.-L.; Chaudhuri, P.; Weyhermüller, T.; Wieghardt, K. Molecular and electronic structure of square planar complexes $[Pd^{II}(^{t}bpy)(L^{IPN,O})]^{0}$, $[Pd^{II}(^{t}bpy)(L^{ISQN,O})](PF_6)$, and $[Pd^{II}(^{t}bpy)(L^{IBQN,O})](PF_6)(BF_4)\cdot 2CH_2Cl_2$: An o-iminophenolato based ligand centered, three-membered redox series. *Dalton Trans.* **2007**, *3*, 373–378. [CrossRef]
28. BaniKhaled, M.O.; Becker, J.D.; Koppang, M.; Sun, H. Perfluoroalkylation of Square-Planar Transition Metal Complexes: A Strategy To Assemble Them into Solid State Materials with a π–π Stacked Lamellar Structure. *Cryst. Growth Des.* **2016**, *16*, 1869–1878. [CrossRef]
29. Tahara, K.; Ashihara, Y.; Higashino, T.; Ozawa, Y.; Kadoya, T.; Sugimoto, K.; Ueda, A.; Morib, H.; Abe, M. New π-extended catecholato complexes of Pt(ii) and Pd(ii) containing a benzothienobenzothiophene (BTBT) moiety: Synthesis, electrochemical behavior and charge transfer properties. *Dalton Trans.* **2019**, *48*, 7367–7377. [CrossRef]
30. Heinze, K.; Reinhardt, S. Platinum(II) Complexes with Non-Innocent Ligands: Solid-Phase Synthesis, Redox Chemistry and Luminescence. *Chem. Eur. J.* **2008**, *14*, 9482–9486. [CrossRef]
31. Shavaleev, N.M.; Davies, E.S.; Adams, H.; Best, J.; Weinstein, J.A. Platinum(II) Diimine Complexes with Catecholate Ligands Bearing Imide Electron-Acceptor Groups: Synthesis, Crystal Structures, (Spectro)Electrochemical and EPR studies, and Electronic Structure. *Inorg. Chem.* **2008**, *47*, 1532–1547. [CrossRef] [PubMed]
32. Best, J.; Sazanovich, I.V.; Adams, H.; Bennett, R.D.; Davies, E.S.; Meijer, A.J.H.M.; Towrie, M.; Tikhomirov, S.A.; Bouganov, O.V.; Ward, M.D.; et al. Structure and Ultrafast Dynamics of the Charge-Transfer Excited State and Redox Activity of the Ground State of Mono- and Binuclear Platinum(II) Diimine Catecholate and Bis-catecholate Complexes: A Transient Absorption, TRIR, DFT, and Electrochemical Study. *Inorg. Chem.* **2010**, *49*, 10041–10056. [CrossRef]
33. Sobottka, S.; Nößler, M.; Ostericher, A.L.; Hermann, G.; Subat, N.Z.; Beerhues, J.; Meer, M.B.-v.d.; Suntrup, L.; Albold, U.; Hohloch, S.; et al. Tuning PtII-Based Donor–Acceptor Systems through Ligand Design: Effects on Frontier Orbitals, Redox Potentials, UV/Vis/NIR Absorptions, Electrochromism, and Photocatalysis. *Chem. Eur. J.* **2020**, *26*, 1314–1327. [CrossRef]

34. Maleeva, A.V.; Ershova, I.V.; Trofimova, O.Y.; Arsenyeva, K.V.; Yakushev, I.A.; Piskunov, A.V. Near-IR absorbing donor-acceptor charge-transfer gallium complex—An example from non-transition metal chemistry. *Mendeleev Commun.* **2022**, *32*, 83–86. [CrossRef]
35. Maleeva, A.V.; Trofimova, O.Y.; Ershova, I.V.; Arsenyeva, K.V.; Pashanova, K.I.; Yakushev, I.A.; Cherkasov, A.V.; Aysin, R.R.; Piskunov, A.V. Molecular and electronic structures of paramagnetic gallium complexes with differently charged o-quinone ligands. *Russ. Chem. Bull.* **2022**, *71*, 1441–1452. [CrossRef]
36. Ershova, I.V.; Maleeva, A.V.; Aysin, R.R.; Cherkasov, A.V.; Piskunov, A.V. Effect of crystal packing on charge transfer in the heteroleptic gallium(III) complex. *Russ. Chem. Bull.* **2023**, *72*, 193–201. [CrossRef]
37. Emsley, J. *The Elements*; Clarendon Press: Oxford, UK, 1991.
38. Piskunov, A.V.; Mescheryakova, I.N.; Fukin, G.K.; Cherkasov, V.K.; Abakumov, G.A. Indium(III) complexes with o-iminobenzoquinone in different redox states. *New J. Chem.* **2010**, *34*, 1746–1750. [CrossRef]
39. Piskunov, A.V.; Meshcheryakova, I.N.; Fukin, G.K.; Shavyrin, A.S.; Cherkasov, V.K.; Abakumov, G.A. The new C–C bond formation in the reaction of o-amidophenolate indium(III) complex with alkyl iodides. *Dalton Trans.* **2013**, *42*, 10533–10539. [CrossRef]
40. Piskunov, A.V.; Meshcheryakova, I.N.; Ershova, I.V.; Bogomyakov, A.S.; Cherkasov, A.V.; Fukin, G.K. The reactivity of o-amidophenolate indium(III) complexes towards different oxidants. *RSC Adv.* **2014**, *4*, 42494–42505. [CrossRef]
41. Piskunov, A.V.; Maleeva, A.V.; Fukin, G.K.; Baranov, E.V.; Bogomyakov, A.S.; Cherkasov, V.K.; Abakumov, G.A. Synthesis and molecular structure of indium complexes based on 3,6-di-tert-butyl-o-benzoquinone. Looking for indium(I) o-semiquinolate. *Dalton Trans.* **2011**, *40*, 718–725. [CrossRef] [PubMed]
42. Brown, S.N. Metrical Oxidation States of 2-Amidophenoxide and Catecholate Ligands: Structural Signatures of Metal−Ligand π Bonding in Potentially Noninnocent Ligands. *Inorg. Chem.* **2012**, *51*, 1251–1260. [CrossRef] [PubMed]
43. Perrin, D.D.; Armarego, W.L.F.; Perrin, D.R. *Purification of Laboratory Chemicals*; Pergamon Press: Oxford, UK, 1980.
44. Abakumov, G.A.; Druzhkov, N.O.; Kurskii, Y.A.; Shavyrin, A.S. NMR study of products of thermal transformation of substituted N-aryl-o-quinoneimines. *Russ. Chem. Bull. Int. Ed.* **2003**, *52*, 712–717. [CrossRef]
45. *Rigaku Oxford Diffraction, CrysAlisPro Software System*, ver. 1.171.42.72a. Rigaku Corpo-ration: Wroclaw, Poland, 2022.
46. Sheldrick, G.M. SHELXT-Integrated Space-Group and Crystal-Structure Determination. *Acta Cryst.* **2015**, *A71*, 3–8. [CrossRef] [PubMed]
47. Sheldrick, G.M. Crystal structure refinement with SHELXL. *Acta Cryst.* **2015**, *C71*, 3–8. [CrossRef]